

# Accelerated Real-time Cine and Flow Under In-magnet Staged Exercise

Preethi Chandrasekaran<sup>1</sup>, Chong Chen<sup>1</sup>, Yingmin Liu<sup>2</sup>,  
Syed Murtaza Arshad<sup>3</sup>, Christopher Crabtree<sup>4</sup>, Matthew Tong<sup>5</sup>,  
Yuchi Han<sup>5</sup>, Rizwan Ahmad<sup>1,3\*</sup>

<sup>1</sup>Biomedical Engineering, Ohio State University, Columbus, OH, USA.

<sup>2</sup>Davis Heart and Lung Research Institute, Ohio State University  
Wexner Medical Center, Columbus, OH, USA.

<sup>3</sup>Electrical and Computer Engineering, Ohio State University,  
Columbus, OH, USA.

<sup>4</sup>Kinesiology, Ohio State University, Columbus, OH, USA.

<sup>5</sup>Cardiovascular Medicine, Ohio State University Wexner Medical  
Center, Columbus, OH, USA.

\*Corresponding author(s). E-mail(s): [ahmad.46@osu.edu](mailto:ahmad.46@osu.edu);

Contributing authors: [chandrasekaran.71@osu.edu](mailto:chandrasekaran.71@osu.edu);  
[chong.chen@osumc.edu](mailto:chong.chen@osumc.edu); [yingmin.liu@osumc.edu](mailto:yingmin.liu@osumc.edu); [arshad.32@osu.edu](mailto:arshad.32@osu.edu);  
[crabtree.223@osu.edu](mailto:crabtree.223@osu.edu); [matthew.tong@osumc.edu](mailto:matthew.tong@osumc.edu); [yuchi.han@osumc.edu](mailto:yuchi.han@osumc.edu);

## Abstract

**Background:** Cardiovascular magnetic resonance imaging (CMR) is a well-established imaging tool for diagnosing and managing cardiac conditions. The integration of exercise stress with CMR (ExCMR) can enhance its diagnostic capacity. Despite recent advances in CMR technology, quantitative ExCMR during exercise remains technically challenging due to motion artifacts and limited spatial and temporal resolution.

**Methods:** This study investigated the feasibility of biventricular functional and hemodynamic assessment using real-time (RT) ExCMR during a staged exercise protocol in 24 healthy volunteers. We applied a coil reweighting technique and employed high acceleration rates to minimize motion blurring and artifacts. We further applied a beat-selection technique that identified beats from the end-expiratory phase to minimize the impact of respiration-induced through-plane motion. Additionally, results from six patients were presented to demonstrate clinical feasibility.

**Results:** Our findings indicated a consistent decrease in end-systolic volume and stable end-diastolic volume across exercise intensities, leading to increased stroke volume and ejection fraction. The selection of end-expiratory beats enhanced the repeatability of cardiac function parameters, as shown by scan-rescan tests in nine volunteers. High scores from a blinded image quality assessment indicated that coil reweighting effectively minimized motion artifacts.

**Conclusions:** This study demonstrated the feasibility of RT ExCMR with in-magnet exercise in healthy subjects and patients. Our results indicate that high acceleration rates, coil reweighting, and selection of respiratory phase-specific heartbeats enhance image quality and repeatability of quantitative RT ExCMR.

**Keywords:** cardiac MRI, exercise stress, accelerated imaging

## List of Abbreviations

CMR, cardiovascular magnetic resonance imaging; CS, compressed sensing; LV, left ventricle; RV, right ventricle; EDV, end-diastolic volume; ESV, end-systolic volume; EF, ejection fraction; SV, stroke volume; CO, cardiac output; HR, heart rate; APHR, age-predicted maximal heart rate; NMAE, normalized mean absolute error; CCC, concordance correlation coefficient; AP, arbitrary respiratory phase; EE, end-expiratory phase; Vmax, peak velocity; RT, real-time; AAo, ascending aorta; MPA, main pulmonary artery; NFF, net forward flow; ExCMR, exercise stress CMR; ECG, electrocardiogram; BC, before correction; AC, after correction; BRPE, Borg rating of perceived exertion; UWT, undecimated wavelet transform; BBP, bean bag positioner; bSSFP, balanced steady-state free-precession; GRE, gradient echo; GRO, golden ratio offset; CAVA, Cartesian sampling with variable density and adjustable temporal resolution; R, acceleration rate; SCoRe, sparsity adaptive composite recovery; VENC, velocity encoding gradient

## 1 Introduction

Cardiovascular magnetic resonance imaging (CMR) is an established tool with proven diagnostic and prognostic value. It is considered a gold standard for biventricular volume quantification and detection of myocardial scar [1]. When paired with pharmacological or exercise stress, CMR-based first-pass perfusion can accurately diagnose coronary artery disease [2, 3] by identifying myocardial ischemia [4]. More recently, cardiac stress imaging has emerged as an attractive option to investigate conditions other than ischemic heart disease. For example, myocardial contractile reserve under stress is observed to be a key prognostic factor in cardiomyopathies and heart failure and is independently associated with major cardiovascular events [5, 6].

Stress CMR investigations commonly involve the use of vasodilators or inotropic agents [7], which fail to mimic the hemodynamic alterations or provide the prognostic data associated with physical exercise [8, 9]. CMR with exercise stress (ExCMR) has the ability to correlate symptoms (e.g., shortness of breath) and functional capacity with workload and thus offer a more comprehensive and dynamic assessment of

cardiovascular function. In pulmonary artery hypertension, for example, ExCMR has shown a superior ability to capture dynamic changes in the right heart than any other modality [10].

Several studies have demonstrated the use of CMR immediately after in-room treadmill exercise [11]. In multiple clinical trials, this strategy has demonstrated success in detecting myocardial ischemia [12]. However, MRI-compatible treadmills are not readily available. Moreover, the need to transfer the patient from the treadmill to the MRI scanner not only creates a time delay between peak exercise and imaging but also makes imaging at various stress levels impractical. In contrast, the commercially available ergometers that enable supine exercise on the MRI patient table are more desirable. Several studies have shown the feasibility of out-of-bore exercise using ergometers [13–15], where the subject exercises on the MRI table outside the magnet. Once the target heart rate or exertion level is achieved, the subject is quickly moved into the scanner for imaging. Although more efficient than the treadmill protocol, this approach still suffers from some of the same limitations.

With advances in highly accelerated real-time (RT) imaging, ExCMR with in-magnet exercise has become an increasingly feasible and informative tool for assessing cardiac function under stress conditions. In 2009, Lurz et al. demonstrated the feasibility of accelerated RT ExCMR in 12 healthy subjects with an isotropic spatial resolution of 3 mm [16]. More recently, several other studies have shown the feasibility of RT ExCMR in small cohorts of healthy subjects [17–19] or patients [15, 20]. Collectively, these studies and the technical advances described within highlight the ongoing evolution of ExCMR. However, these studies still suffer from one or more of these limitations: (i) lower acceleration rates leading to poor in-plane spatial resolution ( $> 3$  mm), (ii) long scan times, (iii) smaller number of slices leading to limited coverage, (iv) dependence on electrocardiogram (ECG) which is typically not reliable during exercise, (v) lack of right ventricular quantification, (vi) absence of hemodynamic assessment, (vii) offline processing, (viii) lack of scan-rescan reproducibility, (ix) insufficient suppression of motion artifacts, especially under high-intensity exercise, (x) lack of a staged protocol, and (xi) sensitivity to through-plane motion.

In this study, we demonstrate the feasibility of biventricular hemodynamic and functional assessment of the heart using RT cine and flow data collected during a staged exercise protocol from 24 healthy subjects. More importantly, we present an in-magnet ExCMR protocol along with related data acquisition and processing techniques that address many of the technical limitations identified in recent ExCMR studies. To underline the clinical feasibility of RT ExCMR, we also present results from six patients.

## 2 Methods

### 2.1 Data acquisition

Twenty-eight healthy volunteers over the age of 18 were recruited to participate in an institutional review board-approved ExCMR study. Written informed consent was obtained from each subject. Data from three volunteers were excluded owing to their non-compliance with instructions or incidental findings. As summarized in Table 1,

twenty-five volunteers were imaged on a 3T scanner (MAGNETOM Vida, Siemens Healthcare, Erlangen, Germany) fitted with an in-magnet supine ergometer (MR Ergometer Pedal, Lode, The Netherlands). The imaging protocol included a free-breathing RT short-axis cine stack (11 to 14 slices) covering the whole heart and at least two long-axis cine slices. Additionally, data were collected from two sets of three closely spaced phase-contrast CMR slices for measuring RT flow at the roots of the aortic and pulmonic arteries, as well as from 4D flow imaging with whole-heart coverage. The RT cine data were collected using a balanced steady-state free-precession (bSSFP) sequence, while the data for RT flow and 4D flow were collected using a gradient echo (GRE) sequence. For cine, a pseudo-random Cartesian sampling pattern, called golden ratio offset (GRO) [21], was used for prospective undersampling, while a different Cartesian sampling pattern, called Cartesian sampling with variable density and adjustable temporal resolution (CAVA) [22], was used for RT flow acquisition. GRO avoids large jumps in k-space between two consecutive readouts. This feature is important for avoiding eddy-currents-induced artifacts in bSSFP sequences [23]. In contrast, CAVA does not restrict the size of jumps in k-space but offers the added flexibility of changing the temporal resolution retrospectively. Since GRE sequences are less sensitive to large jumps in k-space, CAVA was used for RT flow. Both RT cine and flow acquisitions were highly accelerated, with the acceleration rates of  $R \geq 8$  and  $R \geq 16$ , respectively. The protocol used to collect data is shown in Figure 1, and the imaging parameters for RT cine and flow are summarized in Table 2.

	Healthy Subjects	Patients
Number	25	6
Age (years)	$28.9 \pm 7.5$	$60.5 \pm 14.2$
Sex (M/F)	16/9	3/3
BMI (kg/m <sup>2</sup> )	$24.6 \pm 4.1$	$31.3 \pm 8.0$
BSA (m <sup>2</sup> )	$1.4 \pm 0.2$	$1.9 \pm 0.2$

**Table 1:** Human subjects characteristics.

Parameter/Sequence	RT Cine	RT Flow
Sequence	bSSFP	GRE
Acquisition time (s/slice)	3 – 6	3 – 6
Acceleration rate	8 – 9	16 – 19
Repetition Time (ms)	2.60 – 3.16	3.58
Echo Time (ms)	1.10 – 1.42	2.13
Spatial Resolution (mm <sup>2</sup> )	$(1.67 - 2.40) \times (1.67 - 2.40)$	$(2.0 - 2.5) \times (2.0 - 2.5)$
Temporal Resolution (ms)	34.8 – 41.6	35.8 – 42.9
Flip Angle (deg)	24 – 45	10
Slice thickness (mm)	6	6
Sampling pattern	Cartesian [21]	Cartesian [22]
Velocity encoding gradient (cm/s)	N/A	100 – 150 (rest), 200 – 300 (stress)

**Table 2:** MRI acquisition parameters for RT cine and RT flow sequences.



After the ergometer was attached to the end of the table, each subject was positioned on the scanning table, with a medium-sized bean bag positioner (BBP) under their upper torso. The subjects were then asked to find a distance where they could pedal the ergometer comfortably without their knees touching the bore or over-extending their legs. Once a comfortable location was identified, their feet were secured to the ergometer pedals using Velcro straps and suction was applied to BBP using a vacuum device to create a firm mold around the upper torso. This mold helped the subjects stay in one position during in-magnetic exercise. Finally, a blood pressure cuff, a finger pulse oximeter, and ECG leads were attached to the subjects to monitor their vital signs during the scan.

After data acquisition at rest, the volunteers were asked to pedal the ergometer at a rate of 60 cycles per minute by matching their cadence to a metronome played through the headphones. The initial workload was set to 20 W and was increased in increments of 20 W to the maximum of 60 W. The same set of sequences was executed at each exercise stage after allowing a ramp-up time of one minute for the heart rate (HR) to stabilize. Each exercise stage lasted for 8 to 10 minutes. Due to exhaustion or leg fatigue, not all subjects were able to complete all three exercise stages. In total, we had  $n = 25$ ,  $n = 24$ ,  $n = 23$ , and  $n = 16$  volunteers at rest, 20 W, 40 W, and 60 W, respectively. In one of the volunteers, an incidental finding during the resting stage of the protocol prompted termination of the experiment after the resting stage. The data from this volunteer was only used in the repeatability study. For a subset of volunteers, we repeated RT cine and flow acquisitions in quick succession (within 10 minutes) at rest ( $n = 11$ ) and at the 40 W exercise stage ( $n = 9$ ) to assess repeatability. This study is focused on the analysis of RT cine and flow images. The data from the 4D flow acquisition will be reported separately [24].

Before starting the exercise, all the volunteers were verbally encouraged to follow the metronome and maintain a steady cadence of 60 cycles per minute. If the cadence was observed to fall well below 60 cycles per minute during the exercise, the volunteers were offered words of encouragement to maintain the cadence to avoid increased resistance at a lower rotational frequency. Upon completing the scan, volunteers were requested to assess their level of exertion during each stage of the exercise using the Borg rating of perceived exertion (BRPE) scale [25]. This scale categorizes exertion into four distinct levels: “no to extremely light exertion” (scores 6–8), “light exertion” (scores 9–12), “somewhat hard to hard” (scores 13–16), and “very hard to maximal exertion” (scores 17–20). It is important to note that the scale’s range from 6 to 20, when multiplied by 10, corresponds closely with HR measurements, underscoring its effectiveness in quantifying exertion levels.

After completing the healthy subject study, six patient volunteers were also imaged on the same 3T scanner; see Table 1. In contrast to the healthy subjects, a 10 W workload increment was employed when the 20 W increase was considered excessively challenging by the patients. The maximum exercise intensity achieved by the six patients was 60 W, 30 W, 40 W, 20 W, 30 W, and 20 W.

## 2.2 Image reconstruction

The image reconstruction for RT cine and flow was performed inline with Gadgetron-based [26] implementation of a CS method, called sparsity adaptive composite recovery (SCoRe) [27]. A key feature of SCoRe is that it automatically adjusts the regularization strengths across multiple sparsifying transforms based on the image content. The data-driven and parameter-free nature of SCoRe makes it a great match for ExCMR, where temporal sparsity can change significantly with the level of exertion. Coil sensitivity maps were estimated using ESPIRiT [28]. In the case of RT cine, three-dimensional undecimated wavelet transform (UWT) was applied to sparsify both the spatial and temporal dimensions. For RT flow, in addition to UWT, temporal principal components [29], inferred after stacking flow-encoded and flow-compensated images, were used as data-driven sparsifying transform. The reconstruction was performed inline on a dedicated GPU workstation equipped with NVIDIA GeForce RTX 3090. For a 6 s per slice acquisition, the reconstruction time was 10 seconds per slice for RT cine and 15 seconds per slice for RT flow.

Utilizing the BBP significantly limited the torso movement. In addition, the subjects were instructed to firmly hold onto the handles connected to the table's rails during the exercise. Despite these measures, periodic bulk motion was observed during paddling in almost all cases. For some subjects, this resulted in significant degradation of image quality due to the temporally varying sensitivity maps of the body coil array. We attempted to use dynamic sensitivity maps, estimated from a sliding window of a small number of frames, but this approach was unsuccessful. Specifically, a smaller window (less than 8 frames) did not yield a fully sampled region of sufficient size or quality for reliable estimation of coil sensitivity maps, while a larger window (greater than 8 frames) introduced artifacts similar to those from time-averaged sensitivity maps. To mitigate these artifacts, we employed our recently proposed coil reweighting method [30], designed to automatically suppress contributions from artifact-inducing coil elements. This preprocessing step is computationally efficient and can be integrated with any reconstruction method, including CS.

## 2.3 Image analysis

For both RT cine and flow imaging, multiple consecutive heartbeats were collected from each slice. Several studies have highlighted the impact of respiration-induced variation in cardiac output quantification, which is attributed to changes in intrathoracic pressure and through-plane motion [31]. This variation is expected to be more pronounced during exercise. To minimize the impact of respiratory motion on cardiac function assessment, heartbeats from the end-expiratory phase were specifically isolated for analysis. The respiratory signal, critical for identifying this phase, was derived from RT images using a recently proposed principal component analysis-based method [32]. For imaging at rest, the ECG and respiratory signals facilitated the isolation of a single end-expiratory beat. Since ECG signal was unreliable during exercise, the extracted respiratory signal was superimposed and displayed at the bottom of the exercise RT image series. A moving white marker highlighted the respiratory location for each frame. This signal served as a reference to manually identify systolic and

diastolic frames from the end-expiratory phase. An illustration is provided in Supporting Movie S1. The steps of isolating the end-expiratory beat (for rest images) and superimposing the respiratory signal (for exercise images) were performed offline.

The DICOM images from the short-axis cine and flow acquisitions from the ascending aorta (AAo) and main pulmonary artery (MPA) were imported into suiteHEART (NeoSoft, Pewaukee, WI, USA) for hemodynamic and cardiac function quantification. For the RT data collected at rest, only one end-expiratory beat was imported. However, for RT data acquired during exercise stress, the entire cine and flow series, superimposed with the respiratory signal, were imported. Analyses were conducted only on expiratory heartbeats, aided by the reference respiratory signal. For an initial cohort of ten volunteers imaged with an acquisition time of 3 s/slice, all effort was made to conduct the analyses on the end-expiratory beat where possible. The protocol was consequently modified to an acquisition time of 6 s/slice to accommodate slower breathing patterns at rest. Biventricular segmentation was initially performed using suiteHEART software and manually adjusted where necessary. The following parameters were derived for cardiac function analysis: left ventricular (LV) and right ventricular (RV) end-diastolic volume (EDV), end-systolic volume (ESV), stroke volume (SV), and ejection fraction (EF). From the flow images, peak velocity (Vmax), net forward flow (NFF), and SV were measured for both major arteries. To account for the exaggerated through-plane motion, three RT flow slices were acquired from AAo and MPA. From the three slices available, a slice closest to but above the aortic valve was used for AAo flow quantification, and a slice closest to the pulmonic valve but away from the bifurcation was used for MPA flow analysis. The HR at rest and during each exercise stage was extracted from both RT cine and flow images and converted to a percentage of the age-predicted maximal heart rate (APHR). Cardiac output (CO), computed from both cine and flow images, was calculated as the product of SV (mL/beat) and HR (beats/min). In repeat imaging at rest and during a 40 W workload, quantification was performed on a heartbeat from an arbitrary respiratory phase (AP) and on a heartbeat from end-expiration (EE).

To analyze the impact of coil reweighting on image quality, RT cine images from patients were scored with and without the reweighting procedure. From each subject, one mid-ventricular short-axis cine slice and two to three long-axis slices were scored by two expert readers on a five-point Likert-type scale (5-excellent, 4-good, 3-adequate, 2-fair, 1-non-diagnostic) in terms of overall image quality.

## 3 Results

### 3.1 Results from healthy subjects

In Figure 2A, the cardiac function parameters extracted from the short-axis RT cine images are displayed, tracing the progression from rest to three stages of exercise for each volunteer. In summary, the EDV remained relatively consistent from rest through the exercise stages in both ventricles. In contrast, the ESV decreased as exercise intensity and HR increased, indicating more vigorous cardiac contractions during exercise stress. Consequently, the SV typically increased under stress, which is consistent with the literature [17]. However, the pattern of increase in SV varied

among volunteers, ranging from a rapid initial rise to plateauing in some, and a more gradual increase in others. The consistent elevation in CO was attributable to the increased SV and HR. Both HR and APHR trends extracted from the cine images (not shown) were similar to the ones extracted from the flow images.

In Figure 2B, the aortic and pulmonic flow parameters, tracked from rest through three stages of exercise for each volunteer, are depicted. The NFF values demonstrate an overall increase with exercise, although this rise is less pronounced compared to the biventricular stroke volumes. However, CO exhibits a similar trend of increasing with exercise intensity. The peak velocities for both arteries also show an upward trend with exercise. Across all volunteers, the maximum heart rates (recorded from cine or flow) ranged from 92 to 152 bpm and the maximum APHR ranged from 46% to 81%. On average, the subjects were able to achieve a maximum APHR value of 70%. The perceived exertion, measured using BRPE, ranged from 6 to 16, with an average value of 9.3. For the subjects who quit before reaching the 60 W workload, the most commonly expressed reasons were shortness of breath, leg fatigue, and overall exhaustion.

Representative cine and flow images at rest and various stages of exercise of a healthy volunteer are shown in Figure 3. The cine images show a clear delineation of the blood-myocardium boundary, with some marginal blurring at 60 W due to the residual motion. The end-systolic frames exhibit stronger contractility, especially at 60 W. The flow images are mostly free of motion artifacts, with the 60 W magnitude images showing marginal blurring. Note that a higher value of velocity encoding gradient (VENC) was used during exercise; therefore, the velocities are scaled differently for images collected during exercise compared to the resting images.

Figure 4 displays the repeat assessment of biventricular functional parameters from RT cine images at rest and the workload of 40 W. Similarly, Figure 5 presents the repeat assessment of hemodynamic parameters from RT flow images at the same conditions. Overall, both AP and EE beats demonstrate a high level of repeatability. However, in terms of the concordance correlation coefficient (CCC) and normalized mean absolute error (NMAE), EE beats show a marginal but consistent improvement over AP beats; see Figure 6. NMAE, inferred from the two repeats,  $x_1$  and  $x_2$ , is calculated as  $NMSE = 100 \times (|x_1 - x_2|) / (\frac{1}{2}|x_1 + x_2|)$ .

### 3.2 Results from patients

The RT cine and flow data were reconstructed from six CMR patients. In all cases, the image quality, after coil reweighting, was deemed adequate to perform cardiac function and hemodynamic quantification. Figure 7 shows biventricular EF and CO values at rest, during exercise, and post-exercise recovery. Due to the differences in the workload increments and widely different exercise capacities, it was not possible to average the data across patients. Except for one patient, where inadequate spatial coverage due to a user error led to LV-RV mismatch, there was a reasonable agreement between CO and EF from LV and RV. The perceived exertion ranged from 6 to 19 on the BRPE scale, with an average value of 9.3. Although less comprehensive compared to the healthy volunteer study, these results indicate the feasibility of implementing ExCMR in a clinical setting.

Figure 8 shows a representative frame from a patient fatigued at the workload of 20 W. Both RT cine images show clear delineation of blood and myocardium during the systolic and diastolic phases. The flow images are also mostly free of artifacts, with the 20 W magnitude image showing slight blurring. The phase images, however, clearly capture the flow in the ascending and descending aorta. Note that a higher value of VENC was used at 20 W; therefore, the velocities are scaled differently in the 20 W image compared to the resting image.

The artifact suppression method based on coil reweighting was applied to all RT cine data. In cases, where cine images had little to no artifact, coil reweighting had minimal impact on the image quality or quantification. However, in cases where image artifacts were severe, image interpretation or quantitative analysis was not feasible without coil reweighting. Figure 9 shows one such example, where images without coil reweighting exhibit severe artifacts, which are mostly mitigated after coil reweighting. As highlighted in Table 3, the reweighting procedure had no significant ( $p = 0.4$ ) impact on the image quality collected at rest but offered a significant improvement ( $p < 0.01$ ) for the images collected during exercise. Also, all images, after coil reweighting, received a score of 3 or higher.

	Rest BC	Rest AC	Exercise BC	Exercise AC
<b>Average Score</b>	4.78	4.85	3.18*	4.40*
<b>Worst Score</b>	3	4	1	3

**Table 3:** Subjective scoring of RT cine both before (BC) and after (AC) coil reweighting. The average was computed over 23 image series and two readers. \*The pairwise difference between BC and AC was statistically significant ( $p < 0.01$ ) for images collected during exercise.

## 4 Discussion

Advancements in ExCMR technology are pivotal for enhancing the diagnosis and management of cardiovascular diseases. Specifically, ExCMR with in-magnet exercise allows dynamic monitoring of quantitative cardiac function during exercise, revealing functional impairments that are not apparent during resting cardiovascular exams. Because breath-holding is generally not feasible during exercise, free-breathing RT imaging is often used to collect data. Technical challenges associated with ExCMR with in-magnet exercise include image quality degradation due to motion artifacts and limited spatial and temporal resolution. In this work, we demonstrate the feasibility of in-magnet ExCMR for measuring biventricular cardiac function and hemodynamics during staged exercise in both healthy subjects and patients.

To ensure adequate spatial and temporal resolutions, we employed high acceleration rates. This was facilitated by variable density Cartesian sampling and parameter-free CS-based inline reconstruction. To further enhance image quality, we applied our recently developed coil reweighting technique that effectively minimizes motion artifacts caused by the physical movement of the MRI receive coils. Additionally, we leveraged our newly proposed technique to extract cardiac and respiratory

signals directly from the imaging data, eliminating the need for ECG or bellows. This technique allows for consistent selection of end-expiratory heartbeats, thereby minimizing the impact of through-plane motion and improving the repeatability of imaging parameters. In summary, we are able to address the aforementioned limitations for in-magnet ExCMR by (i) achieving high acceleration rates of 8–9 in RT cine and 16–18 in RT flow, leading to the spatial resolution of 1.7–2.4 mm for cine and 2–2.5 mm for flow, (ii) reducing scan time such that a full short-axis stack can be acquired in less than two minutes, (iii) providing whole heart coverage, (iv) developing data processing that is independent of ECG, (v) providing biventricular quantification, (vi) yielding hemodynamic assessment, (vii) developing inline image reconstruction, (viii) establishing scan-rescan repeatability, (ix) suppressing motion artifacts by coil reweighting, (x) enabling images across multiple exercise intensities, and (xi) mitigating sensitivity to through-plane motion by using end-expiratory beats for quantification.

With the ability to quantify volumes and function at each stage, we showed that the physiologic changes in cardiac function and hemodynamic parameters from rest through various stages of exercise in healthy individuals are predominately through decreasing in ESV and increasing in HR. The values of ESV, both for LV and RV, consistently decreased with increased contractility under stress. The values of EDV remain relatively stable across different exercise intensities. As a result, both SV and EF gradually increase with exercise. The increase in CO is driven largely by the increase in HR. This biventricular increase is observed in both cine and flow images.

For scan-rescan repeatability, we showed that selecting an EE beat, compared to an AP beat, results in a modest but consistent improvement in repeatability. With the sole exception of MPA CO, NMAE from all parameters from the EE beat is less than 10% (Figure 6). In contrast, the NMAE exceeds the 10% threshold four times for AP. A similar trend is observed in CCC. Relatively poor CCC and NMAE values for MPA CO can be attributed to HR variations between the two repeats and the small sample size.

Finally, we are able to show the impact of coil reweighting on image quality. Without applying coil reweighting, some of the cine images are not interpretable or suitable for quantification. With coil reweighting, most of the artifacts are eliminated. Note, the coil reweighting comes at the cost of suppressing contribution from certain coil elements, which can lead to partial loss of signal in some areas of the image. However, we did not observe a case where the benefit of suppressing artifacts was outweighed by the loss of intensity. As highlighted by scores in Table 3, coil reweighting improved images collected during exercise, without negatively impacting images collected at rest.

The limitations of this study include a small sample size. This particular protocol had an extended exercise duration, primarily driven by the inclusion of 4D flow acquisition at each exercise stage. If limited to RT cine and flow measurements, it is feasible to complete scanning at each stage within three minutes and dramatically shorten the exercise protocol to 15 minutes for a 5-staged exercise protocol similar to the Bruce protocol [33]. The additional limitations include the highest achieved heart rate in the volunteers and patients was 152 bpm and 123 bpm, respectively. Future research directions will include further optimizing the ExCMR protocol and improving temporal resolution to be able to image at maximal exercise.

## 5 Conclusion

In this preliminary study, we demonstrated the feasibility of ExCMR with in-magnet exercise for quantitative cardiac function evaluation in both healthy volunteers and patients, under multi-stage exercise. The highly accelerated RT imaging was facilitated by a parameter-free CS, overcoming the traditional challenges of limited resolution. Additional key innovative aspects of our technique are the incorporation of a coil reweighting technique and the selection of end-expiratory heartbeats, which resulted in significantly improved image quality and enhanced repeatability of cardiac function measurements.

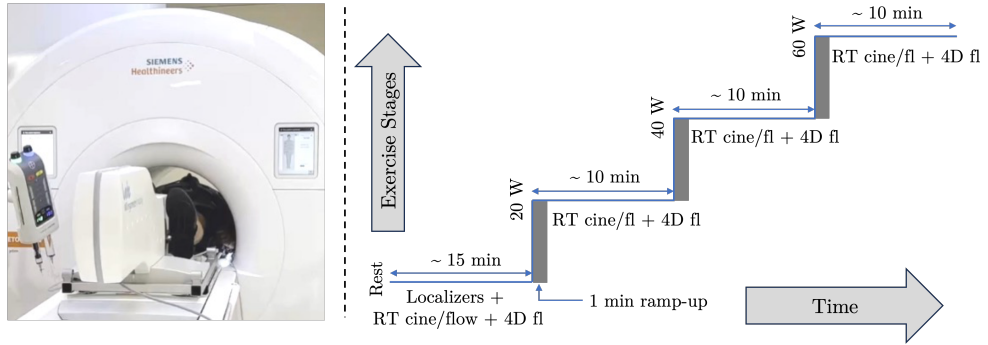


**Fig. 1:** A volunteer exercising inside the MRI bore (left). The multi-stage ExCMR protocol used to scan healthy subjects (right).



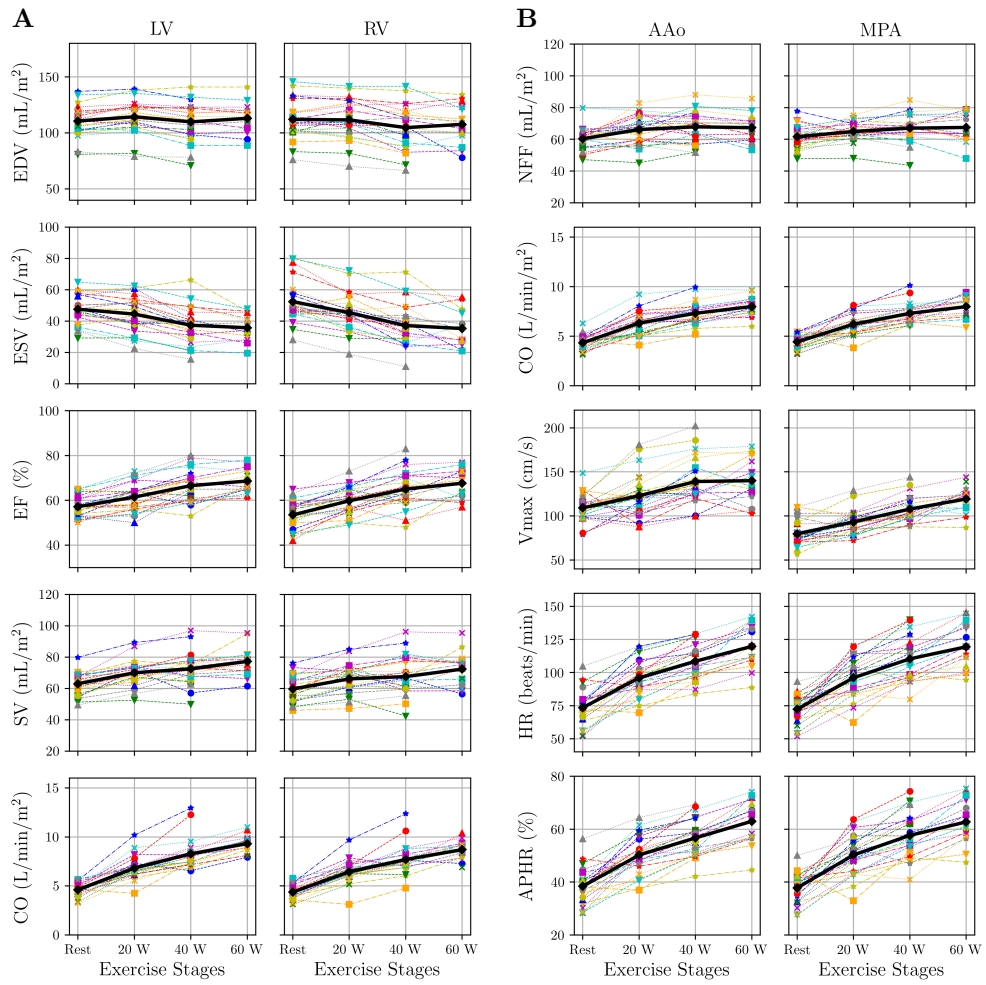


**Fig. 2:** Biventricular cardiac function and hemodynamic assessment from RT cine (A) and RT flow (B). Each trace represents a volunteer, and the thicker black line represents the average value. The HR and APHR values from cine (not shown) were similar to that from flow.

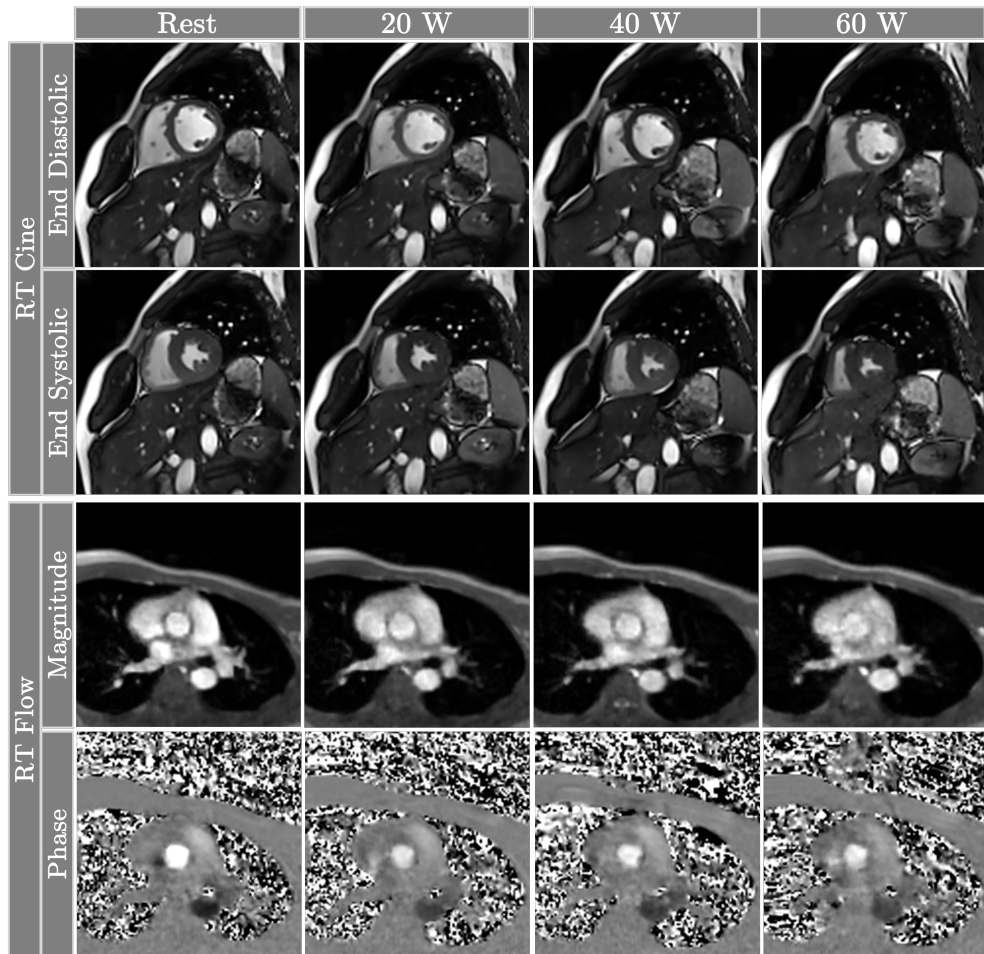


**Fig. 3:** Representative cine and flow frames from a healthy volunteer at rest and across three stages of exercise. Stronger contractility under exercise stress is observed from end-systolic frames (second row). The brighter phase (bottom row) in the resting image is due to the lower value of VENC.

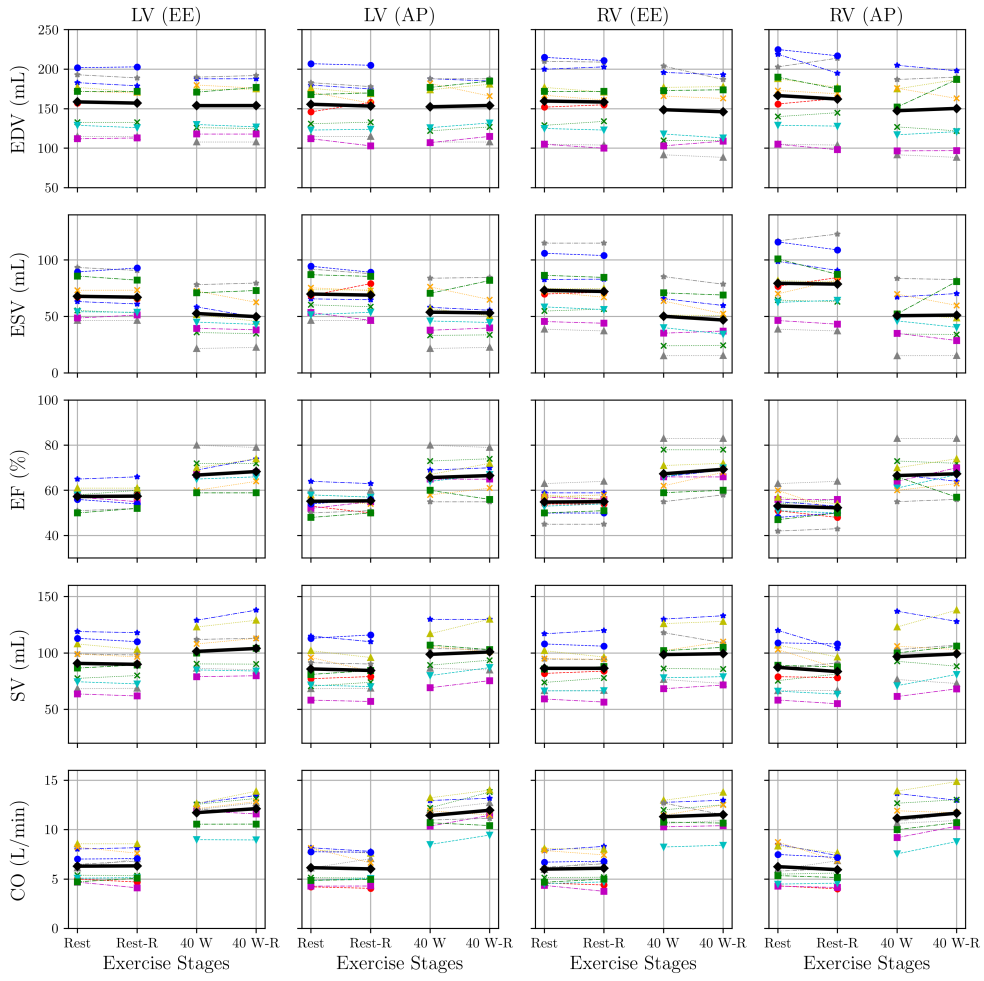


**Fig. 4:** Repeatability of the cine parameters at rest and 40 W for beats from arbitrary respiratory phase (AP) and beats from end-expiratory phase (EE). Here, “Rest-R” and “40 W-R” represent the repeated measurements.

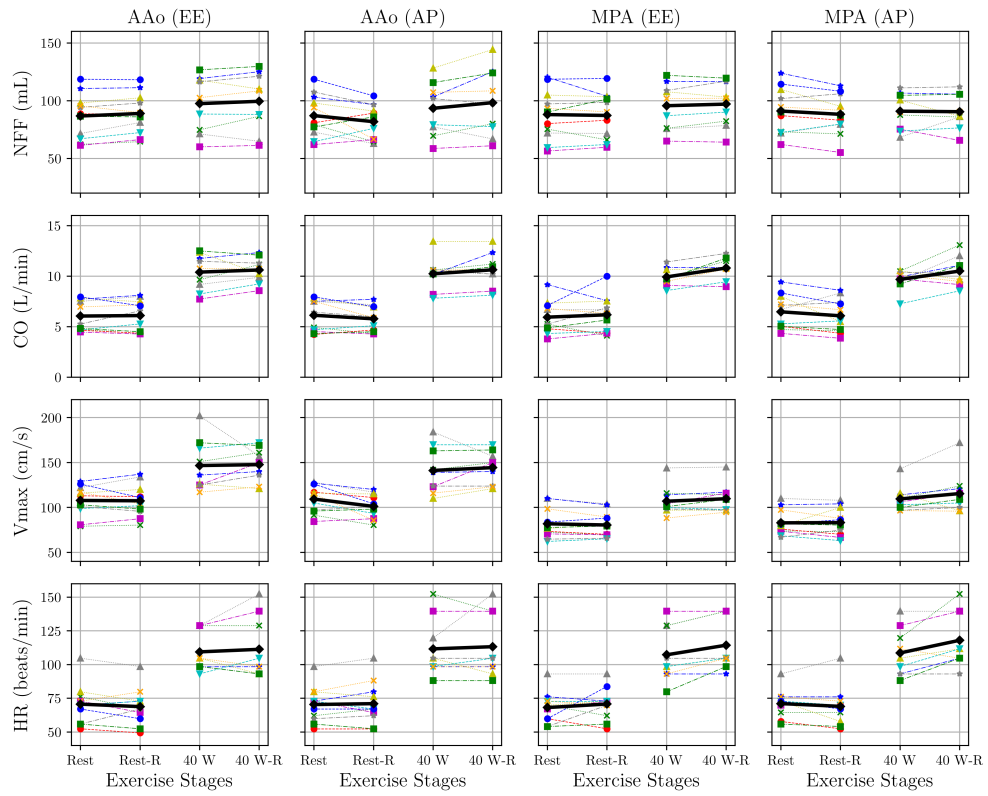


**Fig. 5:** Repeatability of the flow parameters at rest and 40 W for beats from arbitrary respiratory phase (AP) and beats from end-expiratory phase (EE). Here, “Rest-R” and “40 W-R” represent the repeated measurements.

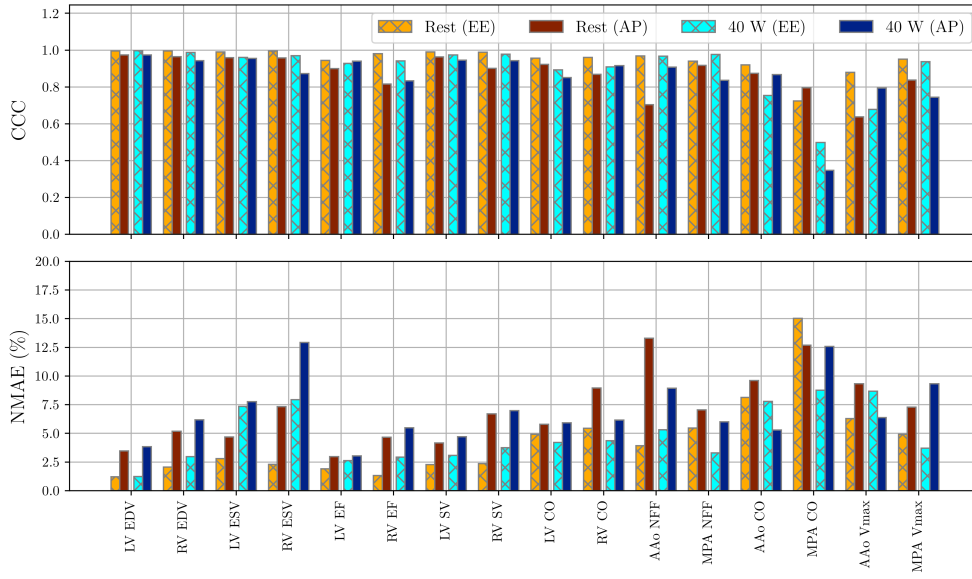


**Fig. 6:** Concordance correlation coefficient (CCC) and normalized mean absolute error (NMAE) for cine and flow parameters for arbitrary respiratory phase (AP) and end-expiratory phase (EE) beats at rest and 40 W.

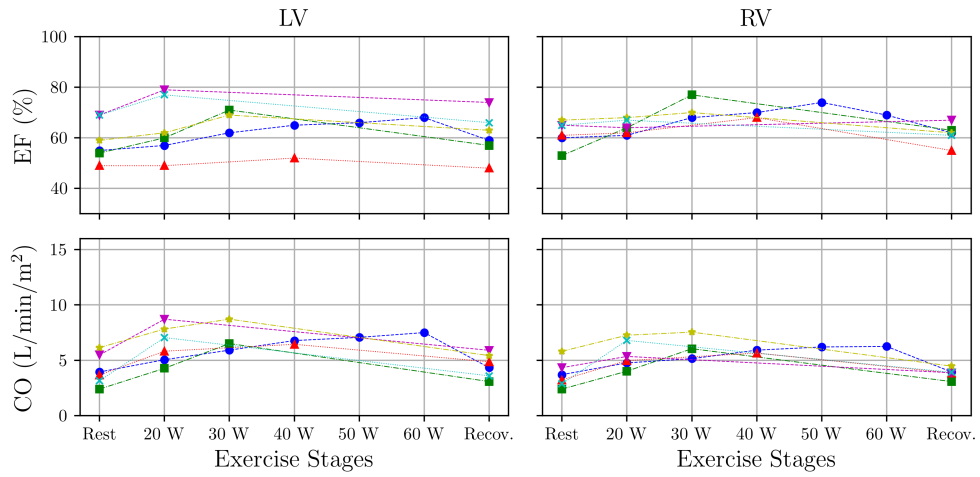


**Fig. 7:** Biventricular cardiac function assessment from RT cine acquired from six patients. The purple trace represents a patient where inadequate LV coverage due to user error led to a discrepancy between RV and LV quantification. Here, “Recov.” represents post-exercise recovery.

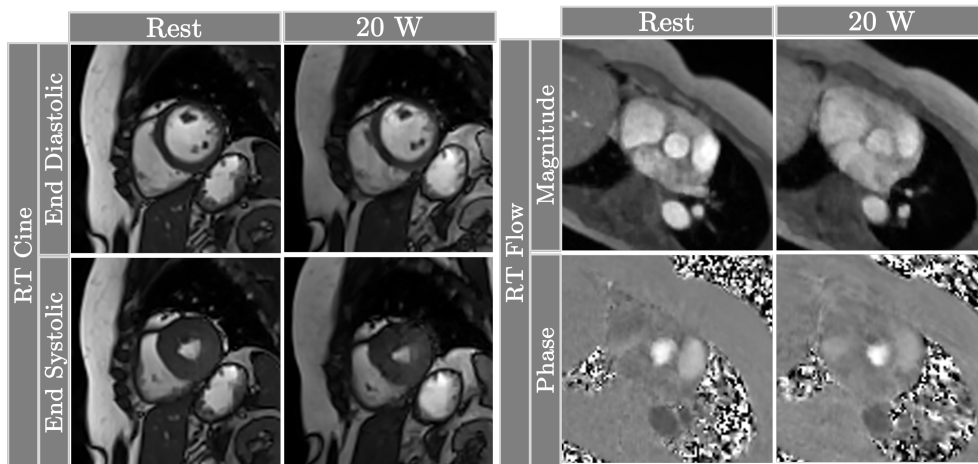


**Fig. 8:** Representative cine and flow frames from a patient at rest and 20 W exercise. Stronger contractility under exercise stress is observed from end-systolic frames. The brighter phase in the resting image is due to the lower value of VENC.

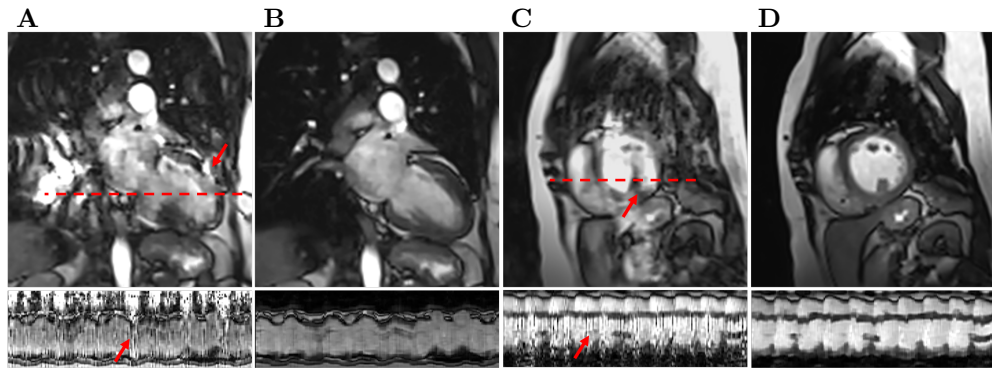


**Fig. 9:** Cine images from one of the patients without coil reweighting (A and C) and with coil reweighting (B and D). Strong motion artifacts are observed in A and C, which are effectively removed in B and D. The images at the bottom represent x-t profile along the dashed red line passing through the heart. The data were collected during exercise at 40 W.



**Supporting Movie S1:** The movie shows a 6 s cine image series from a healthy volunteer collected under 60 W of exercise. The curve at the bottom represents the respiratory motion, with the moving cross representing the current frame.

**Acknowledgments and Funding.** This work was funded by NIH grants R01-EB029957, R01-HL151697, R01-HL148103, and R01-HL135489.

## Ethics Declarations

- **Competing interests:** The authors declare no competing interests.
- **Ethics approval and consent:** For the human subject data, approval was granted by the Institutional Review Board (IRB) at The Ohio State University (2019H0076). Informed consent to participate in the study and to publish results was obtained from all individual participants.
- **Data and code availability:** MRI data and the code to generate results are available upon request
- **Author contribution:** P. Chandrasekaran assisted with data acquisition and processing as well as manuscript writing, C. Chen implemented data processing techniques, Y. Liu assisted with data acquisition and pulse sequence programming, S.M. Arshad assisted with experiment planning, C. Crabtree assisted with subject monitoring during exercise, M. Tong and Y. Han assisted with experiment design and results interpretation, and R. Ahmad supervised all aspects of the study.

## References

- [1] Lima, J.A., Desai, M.Y.: Cardiovascular magnetic resonance imaging: current and emerging applications. *Journal of the American College of Cardiology* **44**(6), 1164–1171 (2004)
- [2] Jong, M.C., Genders, T.S., Geuns, R.-J., Moelker, A., Hunink, M.M.: Diagnostic performance of stress myocardial perfusion imaging for coronary artery disease: a systematic review and meta-analysis. *European Radiology* **22**, 1881–1895 (2012)
- [3] Arai, A.E., Schulz-Menger, J., Shah, D.J., Han, Y., Bandettini, W.P., Abraham, A., Woodard, P.K., Selvanayagam, J.B., Hamilton-Craig, C., Tan, R.-S., *et al.*: Stress perfusion cardiac magnetic resonance vs SPECT imaging for detection of coronary artery disease. *Journal of American College of Cardiology* **82**(19), 1828–1838 (2023)
- [4] Sakuma, H., Suzawa, N., Ichikawa, Y., Makino, K., Hirano, T., Kitagawa, K., Takeda, K.: Diagnostic accuracy of stress first-pass contrast-enhanced myocardial perfusion MRI compared with stress myocardial perfusion scintigraphy. *American Journal of Roentgenology* **185**(1), 95–102 (2005)
- [5] Indorkar, R., Kwong, R.Y., Romano, S., White, B.E., Chia, R.C., Trybula, M., Evans, K., Shenoy, C., Farzaneh-Far, A.: Global coronary flow reserve measured during stress cardiac magnetic resonance imaging is an independent predictor of adverse cardiovascular events. *JACC: Cardiovascular Imaging* **12**(8 Part 2), 1686–1695 (2019)

- [6] Kobayashi, M., Izawa, H., Cheng, X.W., Asano, H., Hirashiki, A., Unno, K., Ohshima, S., Yamada, T., Murase, Y., Kato, T.S., *et al.*: Dobutamine stress testing as a diagnostic tool for evaluation of myocardial contractile reserve in asymptomatic or mildly symptomatic patients with dilated cardiomyopathy. *JACC: Cardiovascular Imaging* **1**(6), 718–726 (2008)
- [7] Kramer, C.M., Barkhausen, J., Bucciarelli-Ducci, C., Flamm, S.D., Kim, R.J., Nagel, E.: Standardized cardiovascular magnetic resonance imaging (CMR) protocols: 2020 update. *Journal of Cardiovascular Magnetic Resonance* **22**(1), 1–18 (2020)
- [8] Leischik, R., Dworak, B., Littwitz, H., Gülker, H.: Prognostic significance of exercise stress echocardiography in 3329 outpatients (5-year longitudinal study). *International Journal of Cardiology* **119**(3), 297–305 (2007)
- [9] Pagnanelli, R.A., Camposano, H.L.: Pharmacologic stress testing with myocardial perfusion imaging. *Journal of Nuclear Medicine Technology* **45**(4), 249–252 (2017)
- [10] Göransson, C., Vejlstrup, N., Carlsen, J.: Exercise cardiovascular magnetic resonance imaging allows differentiation of low-risk pulmonary arterial hypertension. *Journal of Heart and Lung Transplantation* **38**(6), 627–635 (2019)
- [11] Foster, E.L., Arnold, J.W., Jekic, M., Bender, J.A., Balasubramanian, V., Thavendiranathan, P., Dickerson, J.A., Raman, S.V., Simonetti, O.P.: MR-compatible treadmill for exercise stress cardiac magnetic resonance imaging. *Magnetic Resonance in Medicine* **67**(3), 880–889 (2012)
- [12] Raman, S.V., Dickerson, J.A., Mazur, W., Wong, T.C., Schelbert, E.B., Min, J.K., Scandling, D., Bartone, C., Craft, J.T., Thavendiranathan, P., *et al.*: Diagnostic performance of treadmill exercise cardiac magnetic resonance: the prospective, multicenter exercise CMR’s accuracy for cardiovascular stress testing (EXACT) trial. *Journal of the American Heart Association* **5**(8), 003811 (2016)
- [13] Le, T.-T., Bryant, J.A., Ting, A.E., Ho, P.Y., Su, B., Teo, R.C.C., Gan, J.S.-J., Chung, Y.-C., O’Regan, D.P., Cook, S.A., *et al.*: Assessing exercise cardiac reserve using real-time cardiovascular magnetic resonance. *Journal of Cardiovascular Magnetic Resonance* **19**(1), 7 (2016)
- [14] Le, T.-T., Bryant, J.A., Ang, B.W.Y., Pua, C.J., Su, B., Ho, P.Y., Lim, S., Huang, W., Lee, P.T., Tang, H.C., Chin, C.T., Tan, B.Y., Cook, S.A., Chin, C.W.-L.: The application of exercise stress cardiovascular magnetic resonance in patients with suspected dilated cardiomyopathy. *Journal of Cardiovascular Magnetic Resonance* **22**(1), 10 (2020)
- [15] Morales, M.A., Assana, S., Cai, X., Chow, K., Haji-Valizadeh, H., Sai, E., Tsao, C., Matos, J., Rodriguez, J., Berg, S., Whitehead, N., Pierce, P., Goddu, B.,

- Manning, W.J., Nezafat, R.: An inline deep learning based free-breathing ECG-free cine for exercise cardiovascular magnetic resonance. *Journal of Cardiovascular Magnetic Resonance* **24**(1), 1–14 (2022)
- [16] Lurz, P., Muthurangu, V., Schievano, S., Nordmeyer, J., Bonhoeffer, P., Taylor, A.M., Hansen, M.S.: Feasibility and reproducibility of biventricular volumetric assessment of cardiac function during exercise using real-time radial k-t SENSE magnetic resonance imaging. *Journal of Magnetic Resonance Imaging* **29**(5), 1062–1070 (2009)
- [17] Beaudry, R.I., Samuel, T.J., Wang, J., Tucker, W.J., Haykowsky, M.J., Nelson, M.D.: Exercise cardiac magnetic resonance imaging: a feasibility study and meta-analysis. *American Journal of Physiology-Regulatory, Integrative and Comparative Physiology* **315**(4), 638–645 (2018)
- [18] Craven, T.P., Jex, N., Chew, P.G., Higgins, D.M., Bissell, M.M., Brown, L.A.E., Saunderson, C.E.D., Das, A., Chowdhary, A., Dall’Armellina, E., Levelt, E., Swoboda, P.P., Plein, S., Greenwood, J.P.: Exercise cardiovascular magnetic resonance: feasibility and development of biventricular function and great vessel flow assessment, during continuous exercise accelerated by Compressed SENSE: preliminary results in healthy volunteers. *International Journal of Cardiovascular Imaging* **37**, 685–698 (2021)
- [19] Li, Y.Y., Zhang, P., Rashid, S., Cheng, Y.J., Li, W., Schapiro, W., Gliganic, K., Yamashita, A.-M., Grgas, M., Haag, E., Cao, J.J.: Real-time exercise stress cardiac MRI with fourier-series reconstruction from golden-angle radial data. *Magnetic Resonance Imaging* **75**, 89–99 (2021)
- [20] Edlund, J., Haris, K., Ostefeld, E., Carlsson, M., Heiberg, E., Johansson, S., Östenson, B., Jin, N., Aletras, A.H., Steding-Ehrenborg, K.: Validation and quantification of left ventricular function during exercise and free breathing from real-time cardiac magnetic resonance images. *Scientific Reports* **12**(1), 5611 (2022)
- [21] Joshi, M., Pruitt, A., Chen, C., Liu, Y., Ahmad, R.: Technical report (v1.0)–pseudo-random cartesian sampling for dynamic MRI. arXiv preprint arXiv:2206.03630 (2022)
- [22] Rich, A., Gregg, M., Jin, N., Liu, Y., Potter, L., Simonetti, O., Ahmad, R.: Cartesian sampling with variable density and adjustable temporal resolution (CAVA). *Magnetic Resonance in Medicine* **83**(6), 2015–2025 (2020)
- [23] Bieri, O., Markl, M., Scheffler, K.: Analysis and compensation of eddy currents in balanced SSFP. *Magnetic Resonance in Medicine* **54**(1), 129–137 (2005)
- [24] Arshad, S.M., Potter, L.C., Chen, C., Liu, Y., Chandrasekaran, P., Crabtree, C., Tong, M.S., Simonetti, O.P., Han, Y., Ahmad, R.: Motion-robust free-running

- volumetric cardiovascular mri. *Magnetic Resonance in Medicine* (2024)
- [25] Williams, N.: The borg rating of perceived exertion (RPE) scale. *Occupational Medicine* **67**(5), 404–405 (2017)
- [26] Hansen, M.S., Sørensen, T.S.: Gadgetron: an open source framework for medical image reconstruction. *Magnetic Resonance in Medicine* **69**(6), 1768–1776 (2013)
- [27] Chen, C., Liu, Y., Schniter, P., Jin, N., Craft, J., Simonetti, O., Ahmad, R.: Sparsity adaptive reconstruction for highly accelerated cardiac MRI. *Magnetic Resonance in Medicine* **81**(6), 3875–3887 (2019)
- [28] Uecker, M., Lai, P., Murphy, M.J., Virtue, P., Elad, M., Pauly, J.M., Vasanawala, S.S., Lustig, M.: ESPIRiT—An eigenvalue approach to autocalibrating parallel MRI: Where SENSE meets GRAPPA. *Magnetic Resonance in Medicine* **71**(3), 990–1001 (2014)
- [29] Petzschner, F.H., Ponce, I.P., Blaimer, M., Jakob, P.M., Breuer, F.A.: Fast MR parameter mapping using k-t principal component analysis. *Magnetic Resonance in Medicine* **66**(3), 706–716 (2011)
- [30] Chen, C., Liu, Y., Ding, Y., Tong, M., Han, Y., Ahmad, R.: Automatic coil selection to suppress motion artifacts in exercise real-time cine imaging. In: ISMRM ISMRT Annual Meeting Exhibition, Toronto, Canada, p. 1152 (2023)
- [31] Claessen, G., Claus, P., Delcroix, M., Bogaert, J., Gerche, A.L., Heidbuchel, H.: Interaction between respiration and right versus left ventricular volumes at rest and during exercise: a real-time cardiac magnetic resonance study. *American Journal of Physiology-Heart and Circulatory Physiology* **306**(6), 816–824 (2014)
- [32] Chen, C., Chandrasekaran, P., Liu, Y., Simonetti, O.P., Tong, M., Ahmad, R.: Ensuring respiratory phase consistency to improve cardiac function quantification in real-time CMR. *Magnetic Resonance in Medicine* **87**(3), 1595–1604 (2022)
- [33] Bruce, R., Kusumi, F., Hosmer, D.: Maximal oxygen intake and nomographic assessment of functional aerobic impairment in cardiovascular disease. *American Heart Journal* **85**(4), 546–562 (1973)